Single- and Multi-Celled Composite Thin-Walled Beams

Vitali V. Volovoi* and Dewey H. Hodges†

Georgia Institute of Technology, Atlanta, Georgia 30332-0150

A simple composite beam theory that contains only the four "classical" beam variables is constructed from a general variational-asymptotic framework. The results of the theory are contained in closed-form expressions for the stiffness matrices of single- and double-celled composite thin-walled beams. The accuracy of the approach is demonstrated by several examples. The most important feature of these solutions, which distinguishes them from those previously published in the literature, is that shell bending strain measures are consistently taken into consideration. This is shown to be important for correct treatment of certain closed-cell configurations, the torsional stiffness of which can be off by a factor of two when bending strain measures or hoop moments are neglected. Correlation of the present formulae with finite element analysis is demonstrated to be excellent.

Background and Present Approach

Despite the advent of cheap computer power, a simple analytical beam theory can still be quite beneficial for several reasons. First, having more variables in the analysis than necessary can obscure a clear understanding of phenomena being studied. Moreover, preliminary calculations may span a vast design space or interface with other disciplines, which may necessitate keeping the information about the elastic deformation in a maximally compressed form (such as in dynamics, control or aeroelastic analysis of rotorcraft). This paper demonstrates that, contrary to a widespread belief, there is still some room in improving on the existing simple composite beam theories (*i.e.*, the ones that contain only the four "classical" beam variables). Such an improvement can be important, since only when a simple beam theory is free from internal flaws can its comparison with refined theories (*i.e.*, those with a larger number of variables) truly attest to the need of those theories in specific situations.

The following discussion is restricted to the theory of prismatic beams for which the 3-D constitutive law and strain-displacement relationships can be considered linear. Beam theories are associated with the introduction of variables that depend only on the coordinate along the beam axis, which is denoted below as x_1. For a general type of deformation, at least four such 1-D variables have to be introduced: extensional, U_1; torsional, θ; and two bending variables, U_2 and U_3 (corresponding to transverse deflections in two orthogonal directions). The corresponding 1-D governing equations are uncoupled for isotropic beams with doubly symmetric cross sections and correspond to Euler-Bernoulli theory for extension and bending and St.-Venant theory for torsion. When this theory is extended to composite beams, the governing equations become elastically coupled due to the appearance of off-diagonal terms in the cross-sectional stiffness matrix, which we denote by C_{ab}. This 4×4 matrix characterizes the elastic properties of the beam, and the strain energy per unit length is expressed in terms of the four 1-D generalized strain measures as

$$2F_{\text{classical}} = \alpha_a C_{ab} \alpha_b \tag{1}$$

where $\alpha^T = \lfloor U_1' \quad U_2'' \quad U_3'' \quad \theta' \rfloor$ and where ( )′ denotes the derivative with respect to the axial coordinate x_1. For thin-walled beams this problem was first posed in Ref. 1. However, the approach employed therein led to a complicated set of equations, especially in the case of closed cross sections. The solution of those equations was presented only for a special type of 3-D constitutive equations.

The introduction of the variational-asymptotic method in context of anisotropic beams[2] allowed for the treatment of this problem from a different perspective: without making any *ad hoc* assumptions, beam theory can be obtained from 3-D elasticity by making use of the small parameter $\frac{a}{\ell} \ll 1$. Here a is a characteristic dimension of the cross section, and ℓ is the wavelength of deformation along the beam reference line.

For a general cross section the problem is reduced to a system of 2-D equations on a cross section. The development of a numerical solution to this problem is presented in Ref. 3. This solution renders results that correlate very well with those of the numerical procedure outlined in Ref. 4, which relies on the equilibrium equations. Both procedures are based on 2-D finite element cross-sectional discretization and, when the cross-sectional stiffness constants and recovering relations are used in beam theory, the results correlate very well with 3-D elasticity and finite element solutions.

When applying the variational-asymptotic procedure to thin-walled cross sections, one can take advantage of another small parameter, $\frac{h}{a} \ll 1$, where h is a wall thickness. When the asymptotic procedure with respect to $\frac{h}{a}$ is applied directly to the 2-D cross-sectional problem, in some cases solutions can be obtained in closed form for the cross-sectional elastic constants. As opposed to starting with 3-D elasticity, one can also start with shell theory. Rather than having to solve a 2-D problem over the cross-sectional plane, one instead solves a 1-D problem over the contour of the thin walls. Both approaches lead to the same final results, but the latter procedure is much simpler algebraically.

The latter procedure was used in Refs. 5 and 6 to obtain analytical solutions for closed single- and double-celled sections, respectively. The resulting cross-sectional stiffness formulas published in that paper are easy to use and they provide reasonable results for most thin-walled beams. However, shell bending strain measures were neglected in those papers. Similar final formulae can also be obtained from Ref. 7, where equilibrium equations were employed and only shell membrane strain measures were considered as well. An alternative way of treating bending strain measures is to employ the thin-walled beam analog of the uniaxial stress hypothesis, which sets hoop stress resultants and hoop moments to zero (for example, see Refs. 8–11). For most layups all of these theories render practically identical results, which might explain why the deficiency of those theories described in this paper was not realized earlier. However, as shown below, for certain material properties the deviation of all those results from the asymptotically correct results might be significant. Finally, a general procedure was provided in Ref. 12 that allows one to obtain the results presented here.
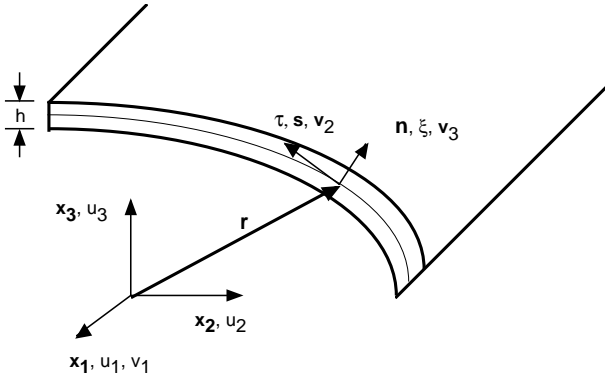
Fig. 1   Configuration and Coordinate system

Solution for Single Cell

In order to employ shell theory for thin-walled beams that have cross sections with curved contours, we introduce R, the characteristic radius of curvature of the undeformed shell mid-surface. Next, we assume $h << a, R$ and make no assumptions about the relative orders of a and R. The cross-sectional Cartesian coordinates are x_2 and x_3. Also, a curvilinear system of cross-sectional coordinates is introduced (see Fig. 1) with ξ and s being the through-thickness and contour coordinates, respectively. In the analysis that follows, vectors are denoted in bold type. With $\mathbf{r} = x_i\mathbf{x}_i$ representing a position vector to the shell midsurface, the notation to be used is

$$(\dot{}\,) \equiv \frac{d(\,)}{ds} \qquad (\,)' \equiv \frac{d(\,)}{dx_1}$$
$$R = \dot{x}_2/\ddot{x}_3 = -\dot{x}_3/\ddot{x}_2$$
$$\boldsymbol{\tau} = \dot{\mathbf{r}} = \dot{x}_2\mathbf{x}_2 + \dot{x}_3\mathbf{x}_3 \qquad (2)$$
$$\mathbf{n} = \boldsymbol{\tau} \times x_1 = \dot{x}_3\mathbf{x}_2 - \dot{x}_2\mathbf{x}_3$$
$$r_\tau = \boldsymbol{\tau} \cdot r = \dot{x}_2 x_2 + \dot{x}_3 x_3$$
$$r_n = \mathbf{n} \cdot \mathbf{r} = x_2\dot{x}_3 - x_3\dot{x}_2$$

Curvilinear displacements v_i are expressed in terms of Cartesian displacements u_i as

$$v_1 = u_1$$
$$v_2 = u_2\dot{x}_2 + u_3\dot{x}_3 \qquad (3)$$
$$v_3 = u_2\dot{x}_3 - u_3\dot{x}_2$$

where index 1 refers to the coordinate along the axis of the beam, index 2 to the (curvilinear) contour coordinate, and index 3 to the through-thickness coordinate. The beam is considered as a cylindrical shell, so that that there are six shell strain measures:[13–15]

$$\gamma_{11} = v_{1,1} \qquad \rho_{11} = v_{3,11}$$
$$2\gamma_{12} = v_{1,2} + v_{2,1}$$
$$\rho_{12} = v_{3,12} + \frac{1}{4R}\left(v_{1,2} - 3v_{2,1}\right)$$
$$\gamma_{22} = v_{2,2} + \frac{v_3}{R} \qquad (4)$$
$$\rho_{22} = v_{3,22} - \left(\frac{v_2}{R}\right)_{,2}$$

where the comma refers to the derivative in the appropriate direction, while $\gamma^T = \lfloor \gamma_{11}\ \gamma_{22}\ 2\gamma_{12} \rfloor$ and $\rho^T = \lfloor \rho_{11}\ \rho_{22}\ \rho_{12} \rfloor$ are membrane and bending/twisting shell strain measures, respectively. (The latter are asymptotically equivalent to the three deformed shell curvature measures $\lfloor \kappa_{11}\ \kappa_{22}\ \kappa_{12} \rfloor$.)

The strain energy density of the shell is a quadratic form of membrane and bending measures. Another way to put it is to say that for a generally anisotropic shell, these six strain shell measures are connected with stress resultants $N^T = \lfloor N_{11}\ N_{22}\ N_{12} \rfloor$ and moments $M^T = \lfloor M_{11}\ M_{22}\ M_{12} \rfloor$

in general by a fully populated 6×6 stiffness matrix:

$$2\mathcal{E}_{\text{shell}} = hE_e^{\alpha\beta\gamma\delta}\gamma_{\alpha\beta}\gamma_{\gamma\delta} + h^3 E_b^{\alpha\beta\gamma\delta}y\rho_{\alpha\beta}\rho_{\gamma\delta} +$$
$$+ 2h^2 E_{eb}^{\alpha\beta\gamma\delta}\gamma_{\alpha\beta}\rho_{\gamma\delta} \qquad (5)$$

where Greek indices vary from 1 to 2; $E_e^{\alpha\beta\gamma\delta}$ and $E_b^{\alpha\beta\gamma\delta}$ are 2-D material constants corresponding to membrane and bending deformation, respectively; and $E_{eb}^{\alpha\beta\gamma\delta}$ corresponds to the coupling between these two types of deformation. Explicit formulae for these constants are found in the Appendix.

For the following discussion it is convenient to rewrite Eq. (5) as

$$2\mathcal{E}_{\text{shell}} = \psi_i Q_{ij}\psi_j + 2\phi_i S_{ij}\psi_j + \phi_i P_{ij}\phi_j \qquad (6)$$

where $\psi^T \equiv \lfloor \gamma_{11}\ h\rho_{11}\ h\rho_{12} \rfloor$, and $\phi^T \equiv \lfloor \gamma_{12}\ \gamma_{22}\ h\rho_{22} \rfloor$; $i,j=1,2,3$ and 3×3 matrices Q_{ij}, S_{ij}, and P_{ij} are corresponding combinations of $E_e^{\alpha\beta\gamma\delta}$, $E_{eb}^{\alpha\beta\gamma\delta}$, and $E_b^{\alpha\beta\gamma\delta}$ (explicit expressions for these matrices are given in the Appendix).

Consistently using the above-mentioned small parameters, $\frac{a}{\ell}$ and $\frac{h}{a}$, it follows from application of the variational-asymptotic method[12] that the shell strain measures are functions of the four classical beam variables: three translations $U_i(x_1)$ of a cross section in the x_i direction and one rotation θ of a cross section about x_1. Furthermore, for closed sections, finding the expressions for those shell strain measures leads to the following conclusions: $\gamma_{11} = U_1' - x_2 U_2'' - x_3 U_3''$ is known (and obvious); ρ_{xx} and ρ_{xs} are small and can be neglected (note that the latter term cannot be neglected for open sections), while γ_{xs}, γ_{ss} and ρ_{ss} are unknowns that can be found by minimizing the energy. Since the energy is a quadratic function of the unknowns, this minimization is straightforward. The only subtlety of the analysis stems from the fact that for each cell of the cross section, four constraints must be imposed on the unknowns. These constraints follow from the requirement that the Cartesian displacements and the slope of the contour in the cross-sectional plane be single-valued. Thus, $\Xi \equiv h\widehat{w}_{3,2} - h\widehat{w}_2/R$, so that $\Xi_{,2} = \phi_3$. Clearly $\oint \overline{\phi}_3 ds \equiv \oint \Xi_{,2} ds = 0$. Next, $\oint u_{1,2} ds = \oint \widehat{w}_{1,2} ds = 0$, so that $\oint \overline{\phi}_1 ds = \theta' \oint r_n ds$. The other two constraints are a bit less straightforward. However, as shown in Ref. 12 the requirement that the two in-plane Cartesian coordinates u_2 and u_3 be single-valued is equivalent to

$$\oint \dot{x}_\alpha \Xi ds = 0 \quad \text{or} \quad \oint x_\alpha \phi_3 ds = 0 \qquad (7)$$

Therefore, for a single-cell cross section, the functional to be minimized has the form

$$2\Lambda = \oint \left[\overline{\psi}_1^2 Q_{11} + 2\overline{\phi}_i S_{i1}\overline{\psi}_1 + \overline{\phi}_i P_{ij}\overline{\phi}_j + \right.$$
$$\left. + 2\lambda_1(\overline{\phi}_1 + \theta' r_n) + 2\overline{\phi}_3(\lambda_\alpha x_\alpha + \lambda_4) \right] ds \qquad (8)$$

where λ_a are Lagrange multipliers; here and below $a = 1,\ldots,4$. Then the solution is given by

$$\overline{\phi}_i = -c_i\overline{\psi}_1 - P_{ij}^{-1}t_j \qquad \text{where} \quad c_i \equiv P_{ij}^{-1}S_{j1} \qquad (9)$$

Here $t^T = \lfloor \lambda_1,\ 0,\ (\lambda_\alpha x_\alpha + \lambda_4) \rfloor$.

Recalling that each Lagrange multiplier is a function of the four 1-D generalized strain measures α_a, we can explicitly write a system of 4 linear equations for the Lagrange multipliers: $F\lambda = J\alpha$, so that $\lambda = F^{-1}J\alpha$. The Appendix provides explicit expressions for F and J. After substituting the expression found for the Lagrange multipliers into Eq. (9) and the result into Eq. (8) we obtain the final expression for the strain energy per unit length:

$$2\Lambda = \oint \left[\overline{\psi}_1^2 \left(Q_{11} - S_{i1}P_{ij}^{-1}S_{j1}\right) + t_i P_{ij}^{-1}t_j \right] ds \qquad (10)$$

Table 1   Properties of thin-walled box-beams used in the examples

outer dimensions:	width $a = 0.953$ in
wall thickness: $h = 0.03$	height $b = 0.53$ in
layup:	
right wall CAS1:	$[\theta/-\theta]_3$
upper wall CAS1:	$[\theta]_6$
left wall CAS1:	$[-\theta/\theta]_3$
lower wall CAS1:	$[-\theta]_6$
right and upper walls CAS2:	$[\theta_3/-\theta_3]$
left and lower walls CAS2:	$[-\theta_3/\theta_3]$
right and left walls CAS3:	$[\theta_3/-\theta_3]$
upper and lower walls CAS3:	$[-\theta_3/\theta_3]$
material properties:	$E_l = 20.59 \times 10^6$ psi
$E_t = 1.42 \times 10^6$ psi	$G_{lt} = 8.9 \times 10^5$ psi
$G_{tn} = 6.96 \times 10^5$ psi	$\nu_{lt} = \nu_{tn} = 0.42$

It must be noted that the most computationally intensive aspect of this procedure is the solution of the linear system of equations for the Lagrange multipliers. However, there is no known shortcut for the correct solution, and approximate solutions based on some simplification will inevitably fail for some configurations, as shown below.

Most researchers neglect all shell bending strain measures for closed sections; see, for example, Refs. 5 and 16. This would seem to be logical since ρ_{xs} and ρ_{xx} are small. Moreover, for Circumferentially Uniform Stiffness (CUS) beams, the approach of Ref. 5 yields the results that are practically indistinquishable from the asymptotically correct ones. However, for certain layups, such as those with Circumferentially Asymmetric Stiffness (CAS) construction, ρ_{ss} cannot be neglected without introducing significant errors.

To illustrate this, let us first consider the thin-walled box-beam CAS1, the properties of which are given in Table 1. Note that the normal to each wall is directed outward and from the bottom to the top ply. Experimental results were reported[17] for this box-beam configuration, and analytical theories are customarily correlated against those results.[5,16,18] All analytical solutions are compared to results from VABS, a computer code that performs a 2-D finite element analysis of the cross section[3] as well as SVBT, also a cross-sectional finite element analysis code that is based on the theory developed in Ref. 4. For all cases considered the finite element codes render results that are indistinguishable from each other within plotting precision.

Figs. 2 and 3 show tip bending slope and tip torque, respectively, under the unit shear lead for a cantilevered beam ($l = 30$ in). As can be seen from these figures, considered lay-up is not sensitive to the presence of shell bending strain measures, and all theories yield practically identical results that correlate very well to the numerical results. However, as the following example shows, this is not always the case.

Let us now consider another layup, CAS2 (see Table 1). In the thin-walled approximation, the coupling for this case is negligible, which results in a diagonal 4×4 cross-sectional stiffness matrix. Note the upper curve in Fig. 4, that is calculated using the analysis from Ref. 5, which severely *over*predicts the torsional rigidity.

Although the uniaxial stress hypothesis is asymptotically correct for classical theory of isotropic beams, it can lead to serious errors in the analysis of composite beams.[19] For thin-walled composite beams, for which the analogous assumption is to set $N_{ss} = M_{ss} = 0$, this assumption this is also true. Results for the torsional rigidity are plotted in Fig. 4. These results demonstrate the consequences of this assumption, which are not negligible at all. Indeed, the torsional rigidity is severely *under*predicted when this assumption is invoked for the box-beam CAS2. If we consider a slightly different lay-up CAS3, see Table 1, the situation is similar, but neglecting ρ_{22} leads to even more severe over-
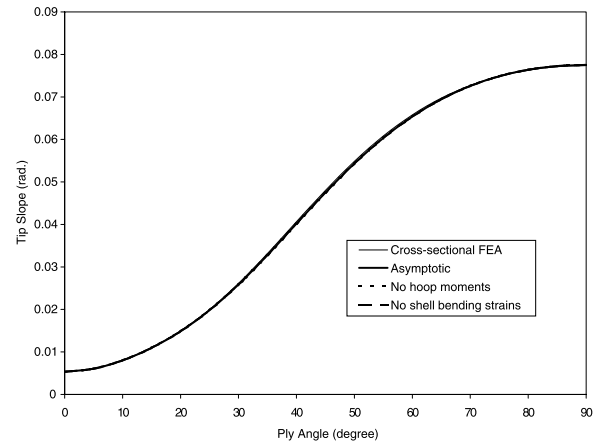
Fig. 2   Tip bending slope under unit shear load, $l = 30$ in
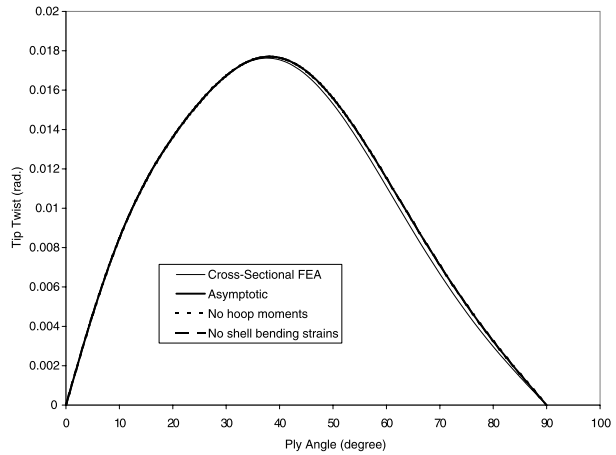
Fig. 3   Tip torque under unit shear load, $l = 30$ in
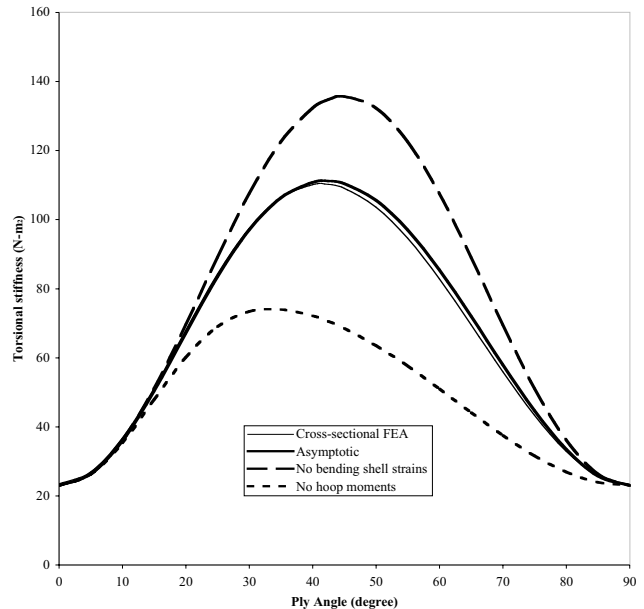
Fig. 4   Torsional Rigidity of Box-Beam, CAS1
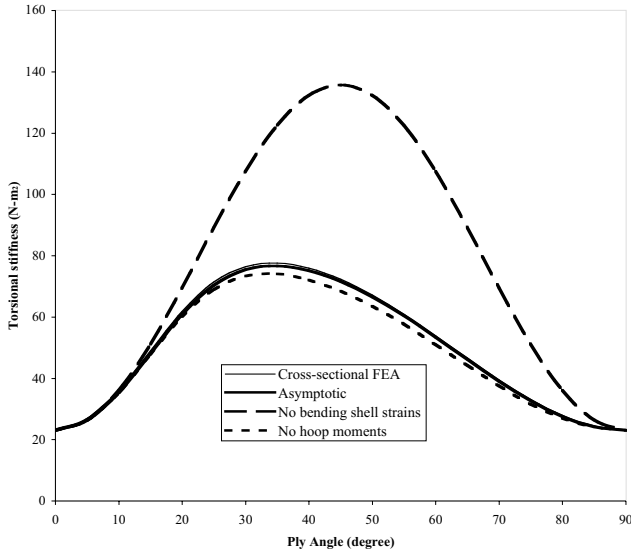
Fig. 5   Torsional Rigidity of Box-Beam, CAS2
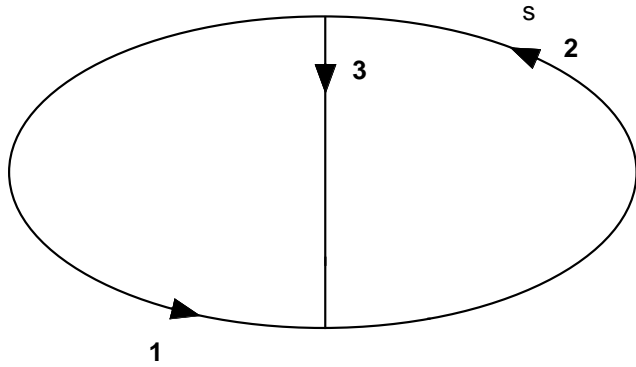
Fig. 6   Direction of integration for a double cell

prediction of the torsional rigidity. According to Fig. 5, for $60°$ it predicts more than twice the actual rigidity. In this particular case, however, setting $N_{ss} = M_{ss} = 0$ does not introduce as large an error.

Double-Cell Formulae

Following the same procedure as the one for a single cell, we have to integrate along the entire contour and introduce four Lagrange multipliers for each cell; therefore, for two cells there will be eight Lagrange multipliers altogether. It must be emphasized that the direction of the integration must be consistent throughout the entire contour. For example, one can choose the direction presented in Fig. 6, and impose constraints over the outside cell $1 + 2$ and the right cell $2+3$. One could reverse the direction of integration over the middle wall and then choose constraints for the outside cell and the left cell, but choosing constraints for left and right cell so that the middle member will be integrated in the opposite direction for the right and left cell respectively will obviously lead to incorrect results. Note that such a convention is different from the one used in traditional textbooks where each cell is treated separately so that no global consistency in the direction of integration is required (see Refs. 20 and 21). Thus, the following constraints must be enforced:

$$\oint_{1+2} \phi_1 ds = \oint_{1+2} \theta' r_n ds \text{ and } \oint_{2+3} \phi_1 ds = \oint_{2+3} \theta' r_n ds$$

$$\oint_{1+2} \phi_3 ds = 0 \text{ and } \oint_{2+3} \phi_3 ds = 0$$

$$\oint_{1+2} x_\alpha \phi_3 ds = 0 \text{ and } \oint_{2+3} x_\alpha \phi_3 ds = 0 \quad (11)$$

and the functional to be minimized has the following form:

$$2\Lambda = \int_{1+2+3} \left[\overline{\psi}_1^2 Q_{11} + 2\overline{\phi}_i S_{i1} \overline{\psi}_1 + \overline{\phi}_i P_{ij} \overline{\phi}_j \right] ds +$$

$$+ \oint_{1+2} \left[2\lambda_1(\overline{\phi}_1 + \theta' r_n) + 2\overline{\phi}_3(\lambda_\alpha x_\alpha + \lambda_4)\right] ds + \quad (12)$$

$$+ \oint_{2+3} \left[2\lambda_5(\overline{\phi}_1 + \theta' r_n) + 2\overline{\phi}_3(\lambda_6 x_2 + \lambda_7 x_3 + \lambda_8)\right] ds$$

Similar to the single-cell case, the solution is given by

$$\overline{\phi}_i = -c_i \overline{\psi}_1 - P_{ij}^{-1} t_j \qquad \text{where } c_i \equiv P_{ij}^{-1} S_{j1} \quad (13)$$

Here, t has a different form for each contour. For contour 1

$$t^T = \lfloor \lambda_1, \ 0, \ \lambda_\alpha x_\alpha + \lambda_4 \rfloor \quad (14)$$

For contour 2

$$t^T = \lfloor \lambda_1 + \lambda_5, \ 0, \ (\lambda_2 + \lambda_6)x_2 + (\lambda_3 + \lambda_7)x_3 + \lambda_4 + \lambda_8 \rfloor \quad (15)$$

and finally, for contour 3

$$t^T = \lfloor \lambda_5, \ 0, \ \lambda_6 x_2 + \lambda_7 x_3 + \lambda_4 \rfloor \quad (16)$$

Recalling that each Lagrange multiplier is a function of four generalized 1-D strain measures α_a, we can explicitly write a system of eight linear equations for the Lagrange multipliers, namely $F_d \lambda = J_d \alpha$, so that $\lambda = F_d^{-1} J_d \alpha$. Matrices F_d and J_d are constructed in exactly in the same fashion as for a single cell: F_d is an 8×8 matrix (the expression for 4×4 matrix $\tilde{F}$ is given in Eq. A.6):

$$F_d = \begin{bmatrix} \oint_{1+2} \tilde{F} ds & \int_2 \tilde{F} ds \\ \int_2 \tilde{F} ds & \oint_{2+3} \tilde{F} ds \end{bmatrix} \quad (17)$$

and J_d is a 4×8 matrix (the expression for the 4×4 matrix $\tilde{J}$ is given in Eq. A.7):

$$J_d = \begin{bmatrix} \oint_{1+2} \tilde{J} ds \\ \oint_{2+3} \tilde{J} ds \end{bmatrix} \quad (18)$$

Substituting the results into Eq. (12), we obtain the final expression for the double-celled strain energy per unit length:

$$2\Lambda = \int_{1+2+3} \left[\overline{\psi}_1^2 \left(Q_{11} - S_{i1} P_{ij}^{-1} S_{j1}\right) + t_i P_{ij}^{-1} t_j\right] ds \quad (19)$$

As a numerical example, consider a double-celled beam. Let us introduce a vertical wall or mid-web in the middle of the box-beam CAS3 with the same width and lay-up as the vertical walls, and see how the torsional rigidity is predicted by the current theory. Qualitatively the situation is similar to the single cell: as expected, there is a very good correlation between the present thin-walled theory and numerical results (see Fig. 7), while both the analysis from Ref. 5 and setting hoop moments to zero result in serious errors. Furthermore, it is remarkable to note that neither of these approximations is sensitive to the introduction of the mid-web at all (see Figs. 5 and 7), while the present
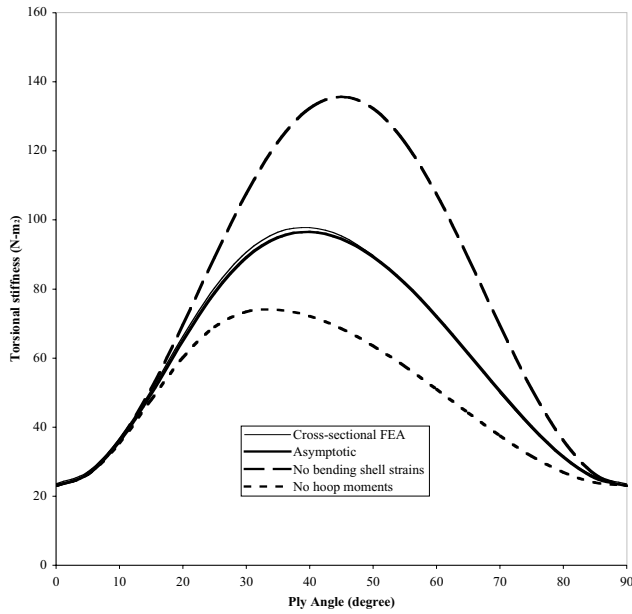
Fig. 7   Torsional rigidity of double cell, dependence on the ply angle

analysis accurately picks up the increase in torsional stiffness due to the mid-web. For comparison, it might be useful to recall a familiar torsional behavior for isotropic beams of the same geometry. In this case, the torsional (St. Venant) warping is out-of-plane and not affected by the presence of the mid-web; indeed, in the thin-walled approximation, the mid-web does not deform when the beam is twisted. Therefore, the torsional rigidity is the same with or without the mid-web. For the anisotropic lay-up under consideration, a totally different situation can be observed from comparison of the displacement fields with and without the mid-web (or 3-D warping) that were obtained numerically using SVBT. In both cases the warping displacement fields are mainly in-plane for this lay-up, and they are clearly affected by the introduction of the mid-web (see Fig. 8). Effectively, the upper and lower walls undergo an in-plane bending, with the mid-web introducing a middle node, which, naturally, leads to an increase in rigidity. It is worth noting that this jump in torsional rigidity is practically independent of the thickness of the web, or of its material properties. Of course, one has to remember that this is true only within the assumptions of linear theory, and in reality the issue of buckling of the mid-web has to be dealt with. Still, the effect is quite remarkable.

Multi-celled sections

Generalizing the formulae for multi-celled sections, it must be recalled that since each cell provides four Lagrange multipliers, the associated system of equations grows unwieldy quite fast. For an N-celled section, the $4N \times 4N$ matrix that has to be inverted has a quite predictable structure: it consists of 4×4 blocks F_{nm} where $n, m = 1, \ldots, N$ with boundaries l_n obtained by integrating $\tilde{F}(s)$ along the boundary of the cell for diagonal blocks and along the common boundary between cell n and cell m for off-diagonal blocks:

$$F_{nm} = \begin{cases} \oint_{l_n} \tilde{F} ds & \text{if } n = m \\ \int_{l_n \cap l_m} \tilde{F} ds & \text{if } n \neq m \end{cases} \quad (20)$$

If two cells do not have a common boundary, then the corresponding 4×4 block consists of zeros, and the solution of this system is more tractable. For example, if we consider a three-celled section in one row (see Fig. 9), then the corre-
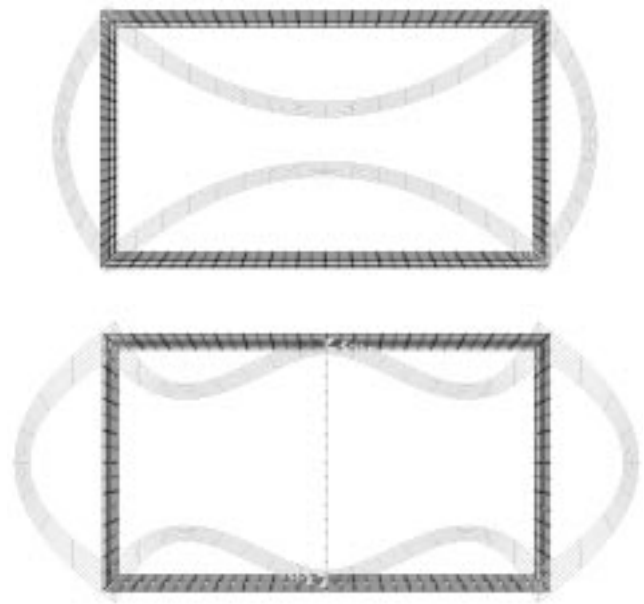
Fig. 8   Cross-sectional displacement fields due to torsion for single (above) and double (below) cells
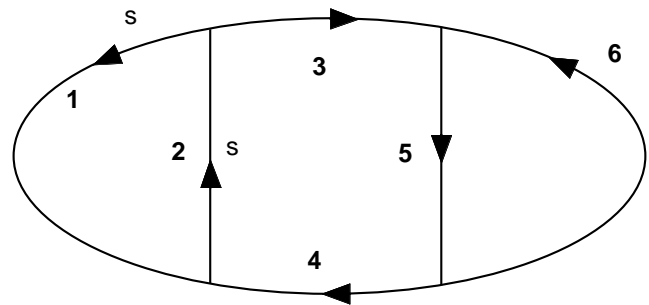
Fig. 9   Direction of integration for three cells

sponding matrix 12×12 F_3 has a banded structure:

$$F_3 = \begin{bmatrix} \oint_{1+2} \tilde{F} ds & \int_2 \tilde{F} ds & 0 \\ \int_2 \tilde{F} ds & \oint_{2+3+4+5} \tilde{F} ds & \int_5 \tilde{F} ds \\ 0 & \int_5 \tilde{F} ds & \oint_{5+6} \tilde{F} ds \end{bmatrix} \quad (21)$$

... and J_3 is 4×12 matrix:

$$J_3 = \begin{bmatrix} \oint_{1+2} \tilde{F} ds \\ \oint_{2+3+4+5} \tilde{F} ds \\ \oint_{5+6} \tilde{F} ds \end{bmatrix} \quad (22)$$

However, there seems to be no shortcut if such common boundaries are present. For example, consider the four-celled section depicted in Fig. 10, in which case the matrix F_4 is 16×16 and not banded, such that

$$F_4 = \begin{bmatrix} \oint_{1+2+5} \tilde{F} ds & \int_2 \tilde{F} ds & 0 & \int_1 \tilde{F} ds \\ \int_2 \tilde{F} ds & \oint_{2+3+6} \tilde{F} ds & \int_3 \tilde{F} ds & 0 \\ 0 & \int_3 \tilde{F} ds & \oint_{3+4+7} \tilde{F} ds & \int_4 \tilde{F} ds \\ \int_1 \tilde{F} ds & 0 & \int_4 \tilde{F} ds & \oint_{1+4+8} \tilde{F} ds \end{bmatrix} \quad (23)$$

Conclusion

A beam theory for thin-walled, multi-celled, anisotropic beams with closed cross sections is constructed based on shell theory. It is shown that local shell bending strain measures can be important for such beams. It is important to
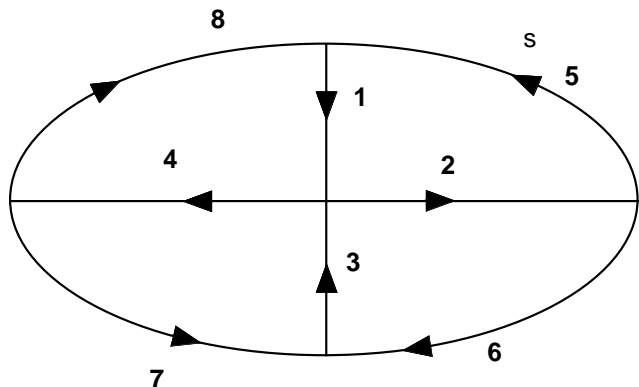
Fig. 10   Direction of integration for four cells

note that, to the best of the authors' knowledge, there are no published analytical theories for such beams that correctly take into account the influence of these strain measures. Explicit formulae for the stiffnesses of single- and double-celled sections are provided, along with examples. The correlation with a finite-element-based solution is excellent. Although the procedure can be applied to N-celled sections, in order to find the formulae for the stiffnesses, one must symbolically invert a $4N \times 4N$ matrix that might be not banded. In this case the analytical solution becomes too cumbersome, and one must resort to a numerical solution of these equations. It must be emphasized that all existing theories involve only one constraint per cell. However, if a correct solution is desired, there seems to be no shortcut to taking all four constraints per cell into consideration. It is useful to note that the "zero shell bending strain" and "zero hoop moment" approximations can be considered as upper and lower bounds, respectively, for the asymptotically correct stiffness constants. Obviously, this leads to a simple spot check for potential errors. If both approximations lead to the same results, then the cross-sectional constants are calculated correctly. However, if there is a significant difference between the two results, then a more accurate procedure is needed. The asymptotic theory derived herein is feasible provided the $4N \times 4N$ matrix can be inverted symbolically. If not, a finite-element-based cross-sectional analysis must be used.

References

[1] Reissner, E. and Tsai, W. T., "Pure Bending, Stretching, and Twisting of Anisotropic Cylindrical Shells," *Journal of Applied Mechanics*, Vol. 39, No. 1, March 1972, pp. 148 – 154.

[2] Berdichevsky, V. L., "On the Energy of an Elastic Rod," *PMM*, Vol. 45, 1982, pp. 518 – 529.

[3] Cesnik, C. E. S. and Hodges, D. H., "VABS: A New Concept for Composite Rotor Blade Cross-Sectional Modeling," *Journal of the American Helicopter Society*, Vol. 42, No. 1, January 1997, pp. 27 – 38.

[4] Borri, M., Ghiringhelli, G. L., and Merlini, T., "Linear Analysis of Naturally Curved and Twisted Anisotropic Beams," *Composites Engineering*, Vol. 2, No. 5-7, 1992, pp. 433 – 456.

[5] Berdichevsky, V. L., Armanios, E. A., and Badir, A. M., "Theory of Anisotropic Thin-Walled Closed-Section Beams," *Composites Engineering*, Vol. 2, No. 5 – 7, 1992, pp. 411 – 432.

[6] Badir, A. M., "Analysis Of Two-Cell Composite Beams," In *Proceedings of the 36rd Structures, Structural Dynamics and Materials Conference*, New Orleans, Louisiana, April 10– 12, 1995, pp. 419–424, AIAA Paper No. AIAA-95-1208-CP.

[7] Mansfield, E. H., "The Stiffness of a Two-Cell Anisotropic Tube," *Aeronautical Quarterly*, May 1981, pp. 338 – 353.

[8] Massa, J. C. and Barbero, E. J., "A Strength of Materials Formulation for Thin Walled Composite Beams with Torsion," *Journal of Composite Materials*, Vol. 32, No. 17, 1998, pp. 1560 – 1594.

[9] Jung, S. N., Nagaraj, V. T., and Chopra, I., "A General Structural Model for Thin- and Thick-Walled Composite Blades with Elastic Couplings," In *Proceedings of the 24th European Rotorcraft Forum*, Marseilles, France, September 15 – 17, 1998, DY-13.

[10] Chandra, R. and Chopra, I., "Structural Response of Composite Beams and Blades with Elastic Couplings," *Composites Engineering*, Vol. 2, No. 5 – 7, 1992, pp. 347 – 374.

[11] Chandra, R. and Chopra, I., "Structural Behavior of Two-Cell Composite Rotor Blades with Elastic Couplings," *AIAA Journal*, Vol. 30, 1992, pp. 2914 – 2921.

[12] Volovoi, V. V. and Hodges, D. H., "Theory of Anisotropic Thin-Walled Beams," *Journal of Applied Mechanics*, Vol. 67, No. 3, Sept. 2000, pp. 453 – 459.

[13] Koiter, W. T., "A Consistent First Approximation in the General Theory of Thin Elastic Shells," In *Proceedings of the IUTAM Symposium. Simposium on the Theory of Thin Elastic Shells*. North-Holland, September 1959, pp. 12–33.

[14] Sanders, J. L., "An Improved First Order Approximmation Theory for Thin Shells," Technical Report 24, NASA, June 1959.

[15] Sanders, J. L., Jr., "Nonlinear Theories for Thin Shells," *Quarterly of Applied Mathematics*, Vol. 21, 1963, pp. 21 – 36.

[16] Johnson, E. R., Vasiliev, V. V., and Vasiliev, D. V., "Anisotropic Thin-Walled Beams With Closed Cross-Sectional Contours," In *Proceedings of the 39th Structures, Structural Dynamics and Materials Conference, Long Beach, California*, April 20 – 23, 1998, pp. 500 – 508, AIAA Paper 98-1761.

[17] Chandra, R., Stemple, A. D., and Chopra, I., "Thin-Walled Composite Beams Under Bending, Torsional, and Extensional Loads," *Journal of Aircraft*, Vol. 27, No. 7, 1990, pp. 619 – 626.

[18] Chandra, R. and Chopra, I., "Experimental and Theoretical Analysis of Composite I-beams with Elastic Coupling," *AIAA Journal*, Vol. 29, No. 12, December 1991, pp. 2197 – 2206.

[19] Volovoi, Vitali V., Hodges, Dewey H., Cesnik, Carlos E. S., and Popescu, Bogdan, "Assessment of Beam Modeling Methods for Rotor Blade Applications," *Mathematical and Computer Modelling*, Vol. 33, No. 10-11, 2001, page 1099 – 1112.

[20] Gjelsvik, A., *The Theory of Thin Walled Beams*, Wiley, New York, New York, 1981.

[21] Megson, T. H. G., *Aircraft Structures for Engineering Students*, Halstead Press, New York, second Edition, 1990.

Appendix

2-D material constants are obtained from the reduced 3-D material constants $D^{\alpha\beta\gamma\delta}$ by use of the relations

$$\left\lfloor E_e^{\alpha\beta\gamma\delta}, \quad E_{eb}^{\alpha\beta\gamma\delta}, \quad E_b^{\alpha\beta\gamma\delta} \right\rfloor =$$
$$= \frac{1}{h} \int_{-h/2}^{h/2} D^{\alpha\beta\gamma\delta} \left\lfloor 1, \quad \frac{\xi}{h}, \quad \left(\frac{\xi}{h}\right)^2 \right\rfloor d\xi \quad \text{(A.1)}$$

These constants are, in turn, obtained from the regular 3-D constants as

$$D^{\alpha\beta\gamma\delta} = E^{\alpha\beta\gamma\delta} - \frac{E^{\alpha\beta33} E^{\gamma\delta33}}{E^{3333}} - H_{\mu\lambda} G^{\alpha\beta\mu} G^{\gamma\delta\lambda}$$

$$\text{where } H_{\mu\lambda}^{-1} = E^{\mu3\lambda3} - E^{\mu333}\frac{E^{\lambda333}}{E^{3333}} \quad \text{(A.2)}$$

$$G^{\alpha\beta\mu} = E^{\alpha\beta\mu3} - \frac{E^{\alpha\beta33}E^{\mu333}}{E^{3333}}$$

Regrouping the strain measures in order to write the energy in the form of Eq. (6) yields the following expressions:

$$Q = h \begin{bmatrix} E_e^{1111} & hE_{eb}^{1111} & 2hE_{eb}^{1112} \\ hE_{eb}^{1111} & h^2 E_b^{1111} & 2h^2 E_b^{1112} \\ 2hE_{eb}^{1112} & 2h^2 E_b^{1112} & 4h^2 E_b^{1212} \end{bmatrix} \quad \text{(A.3)}$$

$$S = h \begin{bmatrix} E_e^{1112} & hE_{eb}^{1112} & 2hE_{eb}^{1212} \\ E_e^{1122} & hE_{eb}^{1122} & 2hE_{eb}^{1222} \\ hE_{eb}^{1122} & h^2 E_b^{1122} & 2h^2 E_b^{1222} \end{bmatrix} \quad \text{(A.4)}$$

$$P = h \begin{bmatrix} E_e^{1212} & E_e^{1222} & hE_{eb}^{1222} \\ E_e^{1222} & E_e^{2222} & hE_{eb}^{2222} \\ hE_{eb}^{1222} & hE_{eb}^{2222} & h^2 E_b^{2222} \end{bmatrix} \quad \text{(A.5)}$$

$$F = \oint \tilde{F} ds \qquad \text{where}$$

$$\tilde{F}(s) = - \begin{bmatrix} P_{11}^{-1} & x_2 P_{13}^{-1} & x_3 P_{13}^{-1} & P_{13}^{-1} \\ & x_2^2 P_{33}^{-1} & x_2 x_3 P_{33}^{-1} & x_2 P_{33}^{-1} \\ & & x_3^2 P_{33}^{-1} & x_3 P_{33}^{-1} \\ Symm & & & P_{33}^{-1} \end{bmatrix} \quad \text{(A.6)}$$

$$J = \oint \tilde{J} ds \qquad \text{where}$$

$$\tilde{J}(s) = \begin{bmatrix} c_1 & -x_2 c_1 & x_3 c_1 & 2r_n \\ x_2 c_3 & -x_2^2 c_3 & -x_2 x_3 c_3 & 0 \\ x_3 c_3 & -x_2 x_3 c_3 & -x_3^2 c_3 & 0 \\ c_3 & -x_2 c_3 & x_3 c_3 & 0 \end{bmatrix} \qquad (\text{A.7})$$